Published in final edited form as:
Mol Oral Microbiol. 2013 October ; 28(5): 342–353. doi:10.1111/omi.12028.

Membrane Association and Destabilization by *Aggregatibacter actinomycetemcomitans* Leukotoxin Requires Changes in Secondary Structures

Michael J. Walters[1,2], **Angela C. Brown**[1,2], **Thomas C. Edrington**[3], **Somesh Baranwal**[1], **Yurong Du**[1], **Edward T. Lally**[1], and **Kathleen Boesze-Battaglia**[4,*]

[1]Department of Pathology, University of Pennsylvania School of Dental Medicine, Philadelphia, PA 19104

[3]Department of Molecular and Cell Biology, University of Connecticut, Storrs, CT 06269

[4]Department of Biochemistry, University of Pennsylvania School of Dental Medicine, Philadelphia, PA 19104

SUMMARY

Aggregatibacter actinomycetemcomitans is a common inhabitant of the upper aerodigestive tract of humans and non-human primates and is associated with disseminated infections, including lung and brain abscesses, pediatric infective endocarditis in children, and localized aggressive periodontitis. *A. actinomycetemcomitans* secretes a repeats-in-toxin protein, leukotoxin, which exclusively kills lymphocyte function-associated antigen-1-bearing cells. The toxin's pathological mechanism is not fully understood; however, experimental evidence indicates that it involves the association with and subsequent destabilization of the target cell's plasma membrane. We have long hypothesized that leukotoxin secondary structure is strongly correlated with membrane association and/or destabilization. In this study, we tested this hypothesis by analyzing lipid-induced changes in leukotoxin conformation. Upon incubation of leukotoxin with lipids that favor leukotoxin-membrane association, we observed an increase in leukotoxin α-helical content that was not observed with lipids that favor membrane destabilization. The change in leukotoxin conformation after incubation with these lipids suggests that membrane binding and membrane destabilization have distinct secondary structural requirements, suggesting that they are independent events. These studies thus provide insight into the mechanism of cell damage that leads to disease progression by *A. actinomycetemcomitans.*

Keywords

Conformation; intrinsic disorder; alpha helix; unordered; lipid membrane

INTRODUCTION

Aggregatibacter actinomycetemcomitans is a common inhabitant of the upper aerodigestive tract of humans and non-human primates. While the bacterium can be recovered from the subgingival sulcus, tongue, buccal mucosa, and the saliva from 10-15% of healthy young individuals (Sirinian *et al.*, 2002), it is also, in certain cases, associated with disseminated

*Correspondence: Dr. Kathleen Boesze-Battaglia, Department of Biochemistry, Levy Building, 240 South 40th St, School of Dental Medicine, University of Pennsylvania, Philadelphia, PA 19104, USA Tel: (+1) 215-898-9167; Fax (+1) 215-898-3695; battagli@upenn.edu.
[2]These authors contributed equally to this work

infections, including lung and brain abscesses (Stepanovic *et al.*, 2005;Hagiwara *et al.*, 2009), pediatric infective endocarditis (Paturel *et al.*, 2004;Tang *et al.*, 2008), and localized aggressive periodontitis (LAP) (Haubek *et al.*, 2008). The organism produces a variety of virulence factors that contribute to either bacterial colonization or pathogenesis of disease. Our interest in the virulence of *A. actinomycetemcomitans* has been focused upon a 114 kDa repeats-in-toxin (RTX) toxin (Coote, 1992), leukotoxin (LtxA), which targets cells involved in both innate and adaptive immune responses. Widely disseminated among Gram-negative bacteria, members of this family share a series of C-terminal glycine-rich repeat units and an ABC-based secretion system, which involves recognition of a signal sequence at the C-terminus of LtxA by membrane-associated proteins and export of the structural toxin gene product directly to the outside of the cell without the participation of a periplasmic intermediate (Fath and Kolter, 1993).

The secretion of LtxA directly into the extracellular milieu poses an interesting enigma, for while it is soluble in an aqueous solution (Lear *et al.*, 2000a;Brogan *et al.*, 1996;Lear *et al.*, 1995a), the protein is also able to interact with and destabilize the lipid bilayer (Brogan *et al.*, 1994;Brown *et al.*, 2012;Lear *et al.*, 1995b;Lear *et al.*, 2000b). Membrane destabilization by LtxA requires the exposure of hydrophobic regions of the protein, which would otherwise be unexposed in water-soluble proteins (Gregory *et al.*, 2011). Therefore, it is proposed that LtxA utilizes a switch between two alternative conformations to achieve biological activity (Lear *et al.*, 1995a;Menestrina *et al.*, 1987;Benz *et al.*, 1989). Similar observations have been made with other water-soluble toxins (Benz *et al.*, 1989;Parker *et al.*, 1989;Choe *et al.*, 1992;Li *et al.*, 1991), whereby hydrophobic residues that are normally sequestered in the interior of the protein undergo a structural reordering upon contact with the membrane.

The molecular flexibility of LtxA upon changes in the temperature or pH as analyzed by tryptophan fluorescence intensity and circular dichroism (CD) (Lear *et al.*, 2000a) has been well documented. The spectra that were generated in those studies did not demonstrate any evidence of a large scale unfolding of LtxA; rather the observed structural modifications were subtle and consistent with the hypothesis that the hydrophobic residues sequestered in the protein interior in the aqueous state became exposed to membrane lipids upon membrane association (Lear *et al.*, 2000a). This observation then led us to originally postulate that LtxA is able to achieve its dichotomous lifestyle through an intrinsically disordered domain (Lally *et al.*, 1999). Other proteins or protein domains (Uversky, 2002;Dunker *et al.*, 2002) that do not form specific 2-D structures under physiological conditions have been documented by analytical methods such as X-ray diffraction, hypersensitivity to protease digestion, and NMR spectroscopy; these techniques have been used to substantiate the presence of segments of intrinsic disorder within these proteins. These regions have been described as natively unfolded, intrinsically unfolded, or intrinsically disordered (Weinreb *et al.*, 1996;Wright and Dyson, 1999;Dunker *et al.*, 2001) based upon their lack of a specific 2-D structural motif.

In the current study, LtxA was incubated with lipid systems to gain insight into the relationship between toxin structure and membrane-dependent cytotoxic properties. We observed strong association of LtxA with single-chain phosphatidylcholine (lysoPC), but previously found no LtxA-induced membrane destabilization with this lipid (Brown *et al.*, 2012). On the other hand, we observed weaker association of LtxA with phosphoethanolamine (PE), but substantial LtxA-induced membrane destabilization (Brown *et al.*, 2012). We therefore used lysoPCs and PEs to study conformational changes in LtxA upon binding and membrane destabilization, respectively. Using a multi-pronged biophysical approach consisting of surface plasmon resonance (SPR), fluorescence spectroscopy, and CD spectroscopy, we investigated changes in LtxA-membrane

interactions and LtxA conformation. We observed that incubation of LtxA with lysoPC, which enhanced protein-lipid association, resulted in an increased α-helical content. This structural change was not observed during incubation of LtxA with PE. We further assessed if calcium (Ca^{2+}), known to bind to LtxA (Lally *et al.*, 1991) induced conformational changes and found that Ca^{2+} does not enhance the lysoPC-induced change in helices. Based on these results, we hypothesize that distinct structural conformations are correlated with LtxA-lipid association and LtxA-induced membrane destabilization, likely in a Ca^{2+}-independent manner.

METHODS

Lipids

1-myristoyl-2-hydroxy-*sn*-glycero-3-phosphocholine (MPC), 1-palmitoyl-2-hydroxyl-sn-glycero-3-phosphocholine (DPC), 1-stearoyl-2-hydroxy-*sn*-glycero-3-phosphocholine (SPC), 1,2-dimyristoyl-*sn*-glycero-3-phosphocholine (DMPC), 1,2-dipalmitoyl-*sn*-glycero-3-phosphocholine (DPPC), 1,2-dimyristoyl-sn-glycero-3-phosphoethanolamine (DMPE), and 1,2-dioleoyl-*sn*-glycero-3-phosphoethanolamine-N-methyl (N-m-DOPE) were purchased from Avanti Polar Lipids (Alabaster, AL) and used without further purification. N-(5-dimethylaminonaphthalene-1-sulfonyl)-1,2-dihexadecanoyl-*sn*-glycero-3-phosphoethanolamine, triethylammonium salt (DANSYL) was purchased from Life Technologies™ (Grand Island, NY).

LtxA preparation

A. actinomycetemcomitans JP2 strain (Tsai *et al.*, 1984) was grown for 48 h at 37°C in *A. actinomycetemcomitans* growth medium (AAGM) (30 g L^{-1} trypticase soy broth, 6 g L^{-1} yeast extract, 8 g L^{-1} dextrose, 0.4% sodium bicarbonate, 5 μg mL^{-1} vancomycin, and 75 μg mL^{-1} bacitracin (Kachlany *et al.*, 2002). The cell culture was centrifuged at 10,100 × g for 15 min at 4 °C to remove cellular debris. Ammonium sulfate (32.5%, mass/volume) was added to the supernatant and precipitation continued under gentle stirring for 2 hours at 4 °C. Precipitates were recovered by centrifugation (10,100 × g for 15 min at 4 °C), resuspended in 10 mM potassium dihydrogen phosphate (pH = 6.5), and then dialyzed against 10 mM potassium dihydrogen phosphate at 4 °C for 40 h. LtxA was then isolated using a HiTrap SP HP ion exchange column with a 5 mL bed volume (GE Healthcare). After the column was loaded and washed with 10 mM potassium dihydrogen phosphate, LtxA was eluted during the second of three isocratic flow regimes of 0.2 M, 0.6 M, and 1.0 M NaCl in 10 mM potassium dihydrogen phosphate. The buffer was then exchanged with 10 mM potassium dihydrogen phosphate (pH = 6.5) (Kachlany *et al.*, 2002).

Liposome preparation

Liposomes were created using the film deposition technique (Olson *et al.*, 1979). Lipids dissolved in chloroform were added to a glass vial in the desired amounts, the chloroform was evaporated under a stream of nitrogen, and the residual chloroform was removed under vacuum. Multilamellar liposomes (MLVs) were formed by hydrating the lipid films with buffer. For the fluorescence spectroscopy, SPR, and CD experiments, the MLVs were extruded 11 times through a 200-nm polycarbonate membrane before use.

Jn.9 cell lipid extract preparation

Jn.9, a subclone of the Jurkat human T lymphoma cell line, was a gift from Dr. Lloyd Klickstein (Cherry *et al.*, 2001). The cells were grown at 37 °C under 5% CO_2 in RPMI 1640 (Mediatech Inc., Herndon, VA) containing 10% fetal calf serum (FCS), 0.1 mM MEM non-essential amino acids, 1× MEM vitamin solution, 2 mM L-glutamine, and 50 μg mL^{-1}

gentamicin. Lipids were extracted from Jn.9 Jurkat cells by adding a 2:1 solution of chloroform:methanol to cell suspensions and vortexing for 2 minutes (extraction was repeated a total of two times). The extracted organic phase was washed with a 0.9% (w/v) NaCl solution and evaporated using a stream of gaseous nitrogen before drying under vacuum (Folch *et al.*, 1957). These extracts consisted of: 16.2% triglycerides, 15.8% cholesterol, 4.9% cholesterol ester, 0.5% cardiolipin, 17.7% phosphotidylethanolamine, 1.6% phosphatidylinositol, 2.1% phosphatidylserine, 35.2% phosphatidylcholine, 6.1% sphingomyelin (lipid analysis reported in weight % and performed by Avanti Polar Lipids, Alabaster, AL).

Förster resonance energy transfer (FRET)

The liposomes for FRET analysis were prepared in 150 mM NaCl, 5 mM $CaCl_2$, 5 mM HEPES, and 3 mM NaN_3, pH 7.4, and were composed of DMPC/MPC (3:1) or DMPC/DMPE (3:1). For both lipid compositions, one set of liposomes contained the FRET acceptor, DANSYL and one did not. The DANSYL composition was set so that the donor (LtxA-Trp)-to-acceptor (DANSYL) ratio was constant (1:18) for all toxin concentrations. Purified LtxA was added to the liposome suspensions at the specified protein:lipid ratios, and the solution was incubated at 37 °C for 30 minutes. The excitation wavelength was set at 295 nm, and the emission intensity was scanned from 310 to 410 nm with the bandpass set to 4 nm. FRET efficiency (%E) was calculated as:

$$\%E = 1 - F_{DA}/F_{D} \quad \text{Eq. 1}$$

where F_D is the fluorescence intensity (measured at 350 nm) of the donor only sample (no DANSYL), and F_{DA} is the fluorescence intensity of the sample containing donor and acceptor. LtxA contains five Trp residues, and it is assumed that all five contribute to the measured %E. Three identical repeats were prepared for each sample type (n=3).

ANTS/DPX Leakage

The ANTS/DPX leakage liposomes were prepared in ANTS/DPX buffer (50 mM NaCl, 25 mM HEPES, 12.5 mM ANTS, 45 mM DPX, pH = 7.4). The dye-encapsulating liposomes were separated from the free dye on a Sephadex G-50 size exclusion column, eluted with a column buffer (50 mM NaCl, 25 mM HEPES, pH = 7.4).

LtxA was added to the ANTS/DPX-encapsulating liposomes in the specified protein:lipid ratio. LtxA-mediated membrane damage was measured by the release of ANTS/DPX (%R):

$$\%R = \frac{I_F - I_B}{I_T - I_B} \quad \text{Eq. 2}$$

where I_F is the fluorescence intensity after toxin addition, I_B is the baseline fluorescence intensity, and I_T is the maximal intensity, obtained after adding 0.1% Triton X-100.

The excitation wavelength was set at 355 nm, and the emission was recorded at 520 nm on a Perkin-Elmer fluorescence spectrometer (LS-55). Passive leakage was accounted for by subtracting the leakage that occurred after addition of buffer (in place of toxin) to ensure that the reported leakage is due only to LtxA.

Tryptophan Intensity

Liposomes composed of DPC or N-m-DOPE were prepared in 150 mM NaCl, 5 mM $CaCl_2$, 5 mM HEPES, and 3 mM NaN_3, pH 7.4, at a lipid concentration of 5 mM. Purified LtxA was added to a cuvette at a concentration of 0.25 mM. A series of 10-μL aliquots of the lipid

stock solution were added individually to the cuvette. After each addition, the sample was allowed to equilibrate at room temperature for 5 min before scanning. The excitation wavelength was set at 280 nm, and the emission was scanned from 300 to 400 nm with bandpasses of 4 nm. The effect of light scattering caused by the addition of liposomes was accounted for by repeating the experiment with buffer only in the cuvette initially. The fluorescence intensity due to liposomes alone was subtracted from the fluorescence intensity due to liposomes and toxin. Two identical repeats were prepared for each sample type (n=2).

Surface Plasmon Resonance

Liposomes composed of DPC or N-m-DOPE (1 mM) were prepared in 150 mM NaCl, 5 mM $CaCl_2$, 5 mM HEPES, and 3 mM NaN_3, pH 7.4, and tethered to an L1 Biacore chip by flowing them over the chip at a rate of 5 μL min^{-1}, until a mass corresponding to approximately 1000 response units (RU) (approximately 5 μL) had been added to the surface (Besenicar and Anderluh, 2010). A small volume of NaOH (5 μL) was added to remove any unbound liposomes. The flow rate was increased to 30 μL min^{-1} before the toxin injection was initiated. Each toxin injection was 60 μL, followed by a 180-μL dissociation injection of buffer alone. The surface was regenerated with an injection of 65 μL 0.5% SDS.

The ten toxin concentrations ranged from 0 nM to 500 nM in a 1:2 dilution series. All SPR measurements were performed on a Biacore® 3000, and the data were evaluated using the BIAevaluation® software. Four identical repeats were prepared for each sample type (n=4). The data were fit using a 1:1 Langmuir binding model to obtain the equilibrium dissociation constant (K_D), as well as the association (k_a) and dissociation (k_d) rates, where K_D is given by:

$$K_D = k_d / k_a \quad \text{Eq. 3}$$

Circular Dichroism Spectroscopy

CD spectroscopy analysis was performed using a Jasco J-810 spectropolarimeter. Samples were prepared in 10 mM phosphate buffer, pH 6.5, with 5 μM LtxA and 2.5 mM lipids, at a protein:lipid molar ratio of 0.0002. In some cases, 1 mM EGTA or 1 mM EGTA plus 10 mM Ca^{2+} was added. Samples were incubated at room temperature for 15 minutes and then analyzed at 25 °C in a 0.2-mm path length quartz cell using the step scanning mode from 260 to 190 nm, with a 1-nm data pitch, 4-s response time, and 1-nm band width. Three independent measurements were collected and averaged for each sample. Three identical repeats were prepared for each sample type (n=3). The LtxA concentration was measured using absorbance at 280 nm and using an extinction coefficient of 82630 M^{-1} cm^{-1}. A Savitzky–Golay smoothing filter was applied to the data with a convolution width of 17. The Dichroweb software (Whitmore and Wallace, 2008) was used, with CDTSTR algorithm and reference set 4 (Compton and Johnson, Jr., 1986;Manavalan and Johnson, Jr., 1987;Sreerama and Woody, 2000) for deconvolution of CD spectra into individual structural components. The mean residue weight, protein concentration, and path length used in these calculations were 108.4 Da, 0.5715 mg mL^{-1}, and 0.2 mm, respectively.

Statistical Analysis

The number of independent repeat experiments is specified in each individual methods subsection. Statistical analysis of the data was performed in Sigmaplot using the t-test. In cases where $p > 0.05$, we reported no statistically significant difference between the two data sets in question.

RESULTS

LtxA association with and destabilization of membranes

LtxA was purified and found to migrate as a single band with a MW of 114 kDa that was immunoreactive with anti-LtxA (LTA-107A_3A_3) (Lally *et al.*, 1999;DiRienzo *et al.*, 1985) (Fig. 1A). The association of LtxA (Fig. 1A) with liposomes of varying lipid compositions was determined by FRET and the kinetics of this association by SPR. Liposomes for the FRET experiment were composed of DMPC in combination with either a PC (MPC) or a PE (DMPE) derivative. The FRET assay takes advantage of energy transfer between Trp (in LtxA) and DANSYL (in liposomes), indicating spatial proximity and association. As shown in Fig. 1B, at lower protein:lipid ratios, the energy transfer between LtxA and liposomes containing either MPC or DMPE was approximately 20%, indicating some LtxA-lipid association. As the LtxA levels increased (protein:lipid ratio increased), the association of LtxA with MPC increased, reaching an energy transfer of 75% while the association of LtxA with DMPE showed no further change. These results suggest that LtxA associates in a dose-dependent manner with liposomes containing the MPC (DMPC/MPC) but not with those containing DMPE (DMPC/DMPE).

To investigate the kinetics of LtxA association with varying lipid types we utilized SPR with two pure lipid systems: a lysolipid, DPC, and a PE, N-m-DOPE. As shown in Table 1 and Fig. 2, the association rate of LtxA to liposomes composed of DPC was substantially faster than the association rate to liposomes composed of N-m-DOPE. In addition, LtxA dissociated much more slowly from liposomes composed of DPC than from liposomes composed of N-m-DOPE. Therefore, the affinity of LtxA (K_D) for DPC is much greater than its affinity for N-m-DOPE. Together, these results suggest that LtxA associates preferentially with DPC over N-m-DOPE.

Once the kinetic parameters of LtxA association with the two different lipid systems were defined, we sought to characterize the membrane disrupting ability of LtxA. Membrane destabilization was measured using a well described 8-aminonaphthalene-1,3,6-trisulfonic acid (ANTS)/p-xylene-bis(N-pyridinium bromide) (DPX) leakage assay. Liposomes composed of either 100% N-m-DOPE or 75% N-m-DOPE/25% DPC were filled with the fluorescent molecule, ANTS, and the quencher, DPX. Because DPC forms pure micelles we compared the LtxA-induced leakage from liposomes composed of N-m-DOPE in the absence and presence of 25% DPC. Membrane damage by LtxA allows dye and quencher to leak from the liposome, resulting in an increase in intensity that is indicative of membrane damage. After 30 min at 37°C, and with a protein:lipid ratios of 0.0002, leakage from liposomes containing N-m-DOPE (% release = 90.26 ± 5.94) is substantially higher than the leakage from liposomes containing N-m-DOPE and DPC (% release = 31.72 ± 4.86).

Collectively, these results suggest that LtxA–lipid association is enhanced in the presence of DPC and MPC. Conversely, LtxA-mediated membrane destabilization is enhanced in liposomes composed of N-m-DOPE. Thus, in the following experiments we investigated the conformational changes in LtxA that occur upon membrane association and destabilization. DPC was used to measure conformational changes associated with binding, and N-m-DOPE was used to measure changes associated with membrane destabilization.

Lipid-induced restructuring of LtxA

Our earlier work demonstrated that a subtle, undefined conformational change in LtxA enhanced its cytotoxic effects, suggesting that the mechanism of LtxA-mediated cytotoxicity may require LtxA to adopt certain conformations. In our current study, we measured Trp fluorescence in the presence of membranes, as a function of lipid:protein ratio, to determine

if conformational changes in LtxA correspond to its membrane association and destabilization functions.

The observed Trp fluorescence intensity in these experiments is due to five Trp residues (Trp-116, Trp-430, Trp-478, Trp-577, and Trp-901) in LtxA. As shown in Table 2, upon LtxA incubation with either DPC or N-m-DOPE for all lipid:protein ratios, a decrease in Trp intensity was observed compared to lipid-free samples (lipid:protein = 0) (Table 2). These results suggest that the LtxA may undergo a conformational change in the presence of these lipids that results in one or more of the Trp residues moving to a more hydrophilic region. In both cases, there was a decrease in Trp intensity at low lipid concentrations, followed by a plateau at higher lipid concentrations. The difference in Trp fluorescence between the two lipid types was not significant at any lipid:protein ratio. To determine the precise nature of the conformational reorganization predicted by Trp quenching studies, CD spectroscopy was used to measure structural components of LtxA in the absence and presence of these lipids.

CD spectra of LtxA

LtxA conformation was determined using CD after incubation with either DPC, N-m-DOPE, or Jn.9 cell lipid extracts (Fig. 3A), and subsequently in the presence of 9 mM Ca^{2+} (Fig. 4A). The spectra were deconvoluted into individual structural components; α-helix, β-sheet, turn, and unordered using Dichroweb (Figs. 3B, 3C, 4B, 4C, & Table 3) (Compton and Johnson, Jr., 1986;Manavalan and Johnson, Jr., 1987;Sreerama and Woody, 2000;Whitmore and Wallace, 2008). CD analysis showed that both DPC and N-m-DOPE induce specific conformations in LtxA; however, the nature of the conformational change is lipid-dependent. Upon incubation with DPC, LtxA adopted a conformation with increased α-helical content, relative to the LtxA-only sample; a similar increase in α-helical content was not detected with N-m-DOPE (Figs. 3B & 3C). Furthermore, the unordered content decreased in LtxA treated with DPC and increased in LtxA treated with N-m-DOPE (Figs. 3B & 3C). When LtxA was preincubated with Ca^{2+}, which is known to bind to LtxA (Lally *et al.*, 1991) and suspected to participate in its pathological mechanism (Fong *et al.*, 2006), in the absence of lipid, α-helical content decreased and unordered content increased (Figs. 4B & 4C). Ca^{2+} preincubation did not change the previously observed DPC-induced increase in α-helices. However, preincubation with Ca^{2+} did affect the lipid-induced structural changes for N-m-DOPE-treated samples, whereby a decrease in α-helices and no change in unordered content were observed (Figs. 4B & 4C).

In the studies, above we utilized a minimalistic approach that did not encompass the complexity of a physiological lipid profile to define how LtxA conformation changed with a functionality, either lipid association or destabilization. To understand how Jn.9 membrane lipids might affect LtxA conformation, LtxA was incubated with lipids extracted from Jn.9 cells. These extracts are composed of lipids from all regions of Jn.9 cells, including but not limited to those on the outer layer of the cell's membrane. Deconvoluted CD spectra from these samples showed decreased α-helical content and increased unordered content compared to LtxA in lipid-free samples (Figs. 3B & 3C).

DISCUSSION

Our previous studies suggest that the mechanism of LtxA cytotoxicity proceeds through two steps: (1) membrane association and (2) membrane destabilization, which occurs through a modification of the bilayer structure (Brown *et al.*, 2012). We found that the association of LtxA to membranes is enhanced in the presence of DPC but not in the presence of N-m-DOPE, which forms membranes that are susceptible to disruption by LtxA (Brown *et al.*, 2012). In this study, we investigated the possibility of lipid effects on LtxA structure and its correlation to membrane association and destabilization. We demonstrated that increased α-

helical content can be correlated to LtxA-membrane association but not to LtxA-mediated membrane destabilization. After incubation with Jn.9 cell lipid extracts, LtxA adopted a conformation with increased turn content and decreased α–helical content (Figs. 3B & 3C), which could be attributed to an interaction with the many lipid types present in the Jn.9 cell lipid extracts. While it seemed possible that increased α-helical content would also be observed in N-m-DOPE-treated samples, because association of LtxA to membrane would precede membrane destabilization, this was not the case. This is likely due to the relatively weak affinity of LtxA to N-m-DOPE, which is 8 orders of magnitude less than that of DPC (K_D values of $2.3e^{-5}\pm0.6e^{-5}$M and $3.8e^{-12}\pm3.4e^{-12}$ M for N-m-DOPE and DPC, respectively).

We demonstrated that LtxA binds preferentially to single-chained phospholipids with a PC headgroup, while bilayer destabilization by LtxA occurs preferentially in lipids with a PE headgroup. In a previous report (Brown, 2012), we demonstrated that bilayer destabilization occurs as a result of a lipid phase change in which the membrane changes from a stable bilayer phase to a less stable, nonlamellar inverted hexagonal (H_{II}) phase. Certain lipids, particularly those with small headgroups (such as PE), and unsaturated acyl chains (such as N-m-DOPE) are more conducive to the formation of the H_{II} phase due to various physical properties. Membrane destabilization through a bilayer-to-H_{II} phase change appears to be a common mechanism used by the RTX toxins (Brown, 2012). Preferential binding to PC lipids is not surprising, as these types of lipids generally comprise a majority of the outer leaflet of eukaryotic cell plasma membranes. We have demonstrated strong binding by LtxA to both single- and double-chained PCs, with strongest binding to single-chained PCs (lysoPCs). We do not know the biophysical reason for this preferential binding, but because single- and double-chained PCs form very different structures, we can hypothesize that the micellar state in which lysolipids reside may be more conducive to LtxA binding than is the bilayer state in which double-chained PCs reside.

The difference in lipid composition between the FRET and SPR experiments is due to technical issues regarding the distribution of fluorescent probes in the liposomes. In both experiments, however, the presence of a lysolipid (DPC or MPC) enhanced binding while the presence of a PE (DMPE or N-m-DOPE) inhibited binding. The agreement of these two experiments demonstrates that this phenomenon is not a lipid-specific effect but is rather due to differences in affinity for different types of lipids (lysolipid vs. PE).

The interactions between LtxA and membranes observed here are consistent with those reported for other members of the RTX family. *Escherichia coli* α-hemolysin (HlyA) undergoes a multiple-step cytotoxic mechanism that includes the reversible adsorption of the toxin to the membrane followed by irreversible insertion of the toxin's acyl chains into the membrane (Bakas *et al.*, 1996). The active form of HlyA contains various regions of intrinsically disordered amino acids that may mediate its pathological mechanism (Herlax and Bakas, 2007;Herlax *et al.*, 2009). In addition, the invasive activity of the *Bordetella pertussis* adenylate cyclase toxin (CyaA) was shown to be associated with a 3% increase in turn content (Cheung *et al.*, 2009). We have shown here that an increase in turn content is associated with nonlamellar phase formation and membrane destabilization, which suggests that the reported invasive activity of CyaA corresponds to the formation of a nonlamellar phase. In fact, CyaA has been shown to induce nonlamellar phase formation (Martin *et al.*, 2004). We have shown that LtxA (and likely the other RTX toxins) induces this nonlamellar phase instead of forming discrete pores and suggested that the formation of this phase may promote toxin translocation (Brown *et al.*, 2012). Interestingly, it was recently reported that the translocation of the enzymatically active (AC) domain of CyaA occurs without the requirement for pore formation (Osickova *et al.*, 2010). Together, these results suggest that

nonlamellar phase induction by RTX toxins promotes translocation without pore formation, and that this process involves a change in the secondary structure of the toxin.

This work has focused on the interaction of LtxA with receptor-free membranes. We and others have shown that LtxA cytotoxicity requires its interaction with a receptor, LFA-1 (Lally *et al.*, 1997;Kieba *et al.*, 2007;Dileepan *et al.*, 2007); however, we have also shown previously (Brown *et al.*, 2012) that LtxA interacts strongly with lipid membranes in the absence of LFA-1. Although this may appear to be counter-intuitive, it is consistent with previous results from our lab and others'. LtxA has been shown to lyse sheep red blood cells, which lack LFA-1, (Balashova *et al.*, 2006), suggesting that it is able to interact directly with the cell membrane when LFA-1 is not present. In addition, we have screened a panel of three monoclonal antibodies and found that while all three inhibit LtxA cytotoxicity, only one inhibits red blood cell lysis (Lally *et al.*, 1994), indicating that at least two separate processes occur during LtxA-mediated cytotoxicity, membrane destabilization (hemolysis/osmolysis), mediated by Epitope A (residues 698-709) and a white blood cell-specific interaction, mediated by Epitopes B (residues 746-757) and C (residues 926-937). Furthermore, evidence from our lab suggests that LtxA binds to both the membrane lipids and LFA-1 with similar affinities, suggesting that LtxA is able to bind both simultaneously (Lally lab/unpublished). We have therefore hypothesized that the membrane-interacting region of LtxA is distinct from the LFA-1-interacting region of LtxA. Here, we have specifically investigated the interaction of LtxA with lipids in the absence of LFA-1 to gain a better understanding of this specific protein-lipid interaction.

Understanding the cytotoxic mechanisms of LtxA and other RTX toxins may provide opportunities for therapeutic intervention in the progression of infectious diseases such as LAP, meningitis, endocarditis, and urogenital infections. Additionally, RTX toxins are attractive candidates for therapeutic applications that require molecules with both aqueous solubility and also the ability to target and interact with lipid membranes. RTX toxins could be classified as specialized membrane-penetrating proteins (Kinyanjui and Fixman, 2008) capable of selecting only the toxin's natural target cells. This therapeutic strategy could avoid interaction with other cell types, reducing the side effects from treatment.

Acknowledgments

We would like to thank Prof. William DeGrado for use of his Jasco J-810 spectropolarimeter, and Yong Ho Kim, Ivan Korendovych, and Patrik Nygren for their insight on CD data interpretation. This project was supported by the National Institutes of Health, National Institute of Dental and Craniofacial Research [5R01DE009517-20 (ETL), 5R01DE022465-02 (KBB), F32DE020950 (ACB), and K99DE022795 (ACB)], the National Eye Institute [5R01EY10420-17 (KBB)], the International Association for Dental Research Microbiology and Immunology Group Travel Award (MJW), and the American Association for Dental Research Bloc Travel Grant (MJW).

Reference List

Bakas L, Ostolaza H, Vaz WL, Goni FM. Reversible adsorption and nonreversible insertion of *Escherichia coli* a-hemolysin into lipid bilayers. Biophys J. 1996; 71:1869–1876. [PubMed: 8889162]

Balashova NV, Crosby JA, Al GL, Kachlany SC. Leukotoxin confers beta-hemolytic activity to Actinobacillus actinomycetemcomitans. Infect Immun. 2006; 74:2015–2021. [PubMed: 16552030]

Benz R, Schmid A, Wagner W, Goebel W. Pore formation by the *Escherichia coli* hemolysin: evidence for an association-dissociation equilibrium of the pore-forming aggregates. Infect Immun. 1989; 57:887–895. [PubMed: 2465272]

Besenicar MP, Anderluh G. Preparation of lipid membrane surfaces for molecular interaction studies by surface plasmon resonance biosensors. Methods Mol Biol. 2010; 627:191–200. [PubMed: 20217622]

Brogan JM, Lally ET, Demuth DR. Construction of pYGK, an Actinobacillus actinomycetemcomitans-Escherichia coli shuttle vector. Gene. 1996; 169:141–142. [PubMed: 8635742]

Brogan JM, Lally ET, Poulsen K, Kilian M, Demuth DR. Regulation of *Actinobacillus actinomycetemcomitans* leukotoxin expression: analysis of the promoter regions of leukotoxic and minimally leukotoxic strains. Infection and Immunity. 1994; 62:501–508. [PubMed: 8300209]

Brown AC, Boesze-Battaglia K, Du Y, Stefano FP, Kieba IR, Epand RF, et al. *Aggregatibacter actinomycetemcomitans* leukotoxin cytotoxicity occurs through bilayer destablization. Cellular Microbiology. 2012; 14:869–881. [PubMed: 22309134]

Cherry LK, Weber KS, Klickstein LB. A dominant Jurkat T cell mutation that inhibits LFA-1-mediated cell adhesion is associated with increased cell growth. J Immunol. 2001; 167:6171–6179. [PubMed: 11714777]

Cheung GY, Kelly SM, Jess TJ, Prior S, Price NC, Parton R, Coote JG. Functional and structural studies on different forms of the adenylate cyclase toxin of *Bordetella pertussis*. Microb Pathog. 2009; 46:36–42. [PubMed: 18992319]

Choe S, Bennett MJ, Fujii G, Curmi PM, Kantardjieff KA, Collier RJ, Eisenberg D. The crystal structure of diphtheria toxin. Nature. 1992; 357:216–222. [PubMed: 1589020]

Compton LA, Johnson WC Jr. Analysis of protein circular dichroism spectra for secondary structure using a simple matrix multiplication. Anal Biochem. 1986; 155:155–167. [PubMed: 3717552]

Coote JG. Structural and functional relationships among the RTX toxin determinants of gram-negative bacteria. FEMS Microbiol Rev. 1992; 8:137–161. [PubMed: 1558765]

Dileepan T, Kachlany SC, Balashova NV, Patel J, Maheswaran SK. Human CD18 is the functional receptor for Aggregatibacter actinomycetemcomitans leukotoxin. Infect Immun. 2007; 75:4851–4856. [PubMed: 17635865]

DiRienzo JM, Tsai CC, Shenker BJ, Taichman NS, Lally ET. Monoclonal antibodies to leukotoxin of Actinobacillus actinomycetemcomitans. Infect Immun. 1985; 47:31–36. [PubMed: 3965404]

Dunker AK, Brown CJ, Lawson JD, Iakoucheva LM, Obradovic Z. Intrinsic disorder and protein function. Biochemistry. 2002; 41:6573–6582. [PubMed: 12022860]

Dunker AK, Lawson JD, Brown CJ, Williams RM, Romero P, Oh JS, et al. Intrinsically disordered protein. J Mol Graph Model. 2001; 19:26–59. [PubMed: 11381529]

Fath MJ, Kolter R. ABC transporters: bacterial exporters. Microbiol Rev. 1993; 57:995–1017. [PubMed: 8302219]

Folch J, Lees M, Sloane Stanley GH. A simple method for the isolation and purification of total lipids from animal tissues. J Biol Chem. 1957; 226:497–509. [PubMed: 13428781]

Fong KP, Pacheco CM, Otis LL, Baranwal S, Kieba IR, Harrison G, et al. *Actinobacillus actinomycetemcomitans* leukotoxin requires lipid microdomains for target cell cytotoxicity. Cell Microbiol. 2006; 8:1753–1767. [PubMed: 16827908]

Gregory SM, Harada E, Liang B, Delos SE, White JM, Tamm LK. Structure and function of the complete internal fusion loop from Ebolavirus glycoprotein 2. Proc Natl Acad Sci U S A. 2011; 108:11211–11216. [PubMed: 21690393]

Hagiwara S, Fujimaru T, Ogino A, Takano T, Sekijima T, Kagimoto S, Eto Y. Lung abscess caused by infection of *Actinobacillus actinomycetemcomitans*. Pediatr Int. 2009; 51:748–751. [PubMed: 19799745]

Haubek D, Ennibi OK, Poulsen K, Vaeth M, Poulsen S, Kilian M. Risk of aggressive periodontitis in adolescent carriers of the JP2 clone of Aggregatibacter (Actinobacillus) actinomycetemcomitans in Morocco: a prospective longitudinal cohort study. Lancet. 2008; 371:237–242. [PubMed: 18207019]

Herlax V, Bakas L. Fatty acids covalently bound to alpha-hemolysin of Escherichia coli are involved in the molten globule conformation: implication of disordered regions in binding promiscuity. Biochemistry. 2007; 46:5177–5184. [PubMed: 17407262]

Herlax V, Mate S, Rimoldi O, Bakas L. Relevance of fatty acid covalently bound to Escherichia coli alpha-hemolysin and membrane microdomains in the oligomerization process. J Biol Chem. 2009; 284:25199–25210. [PubMed: 19596862]

Kachlany SC, Fine DH, Figurski DH. Purification of secreted leukotoxin (LtxA) from *Actinobacillus actinomycetemcomitans*. Protein Expression and Purification. 2002; 25:465–471. [PubMed: 12182827]

Kieba IR, Fong KP, Tang HY, Hoffman KE, Speicher DW, Klickstein LB, Lally ET. Aggregatibacter actinomycetemcomitans leukotoxin requires beta-sheets 1 and 2 of the human CD11a beta-propeller for cytotoxicity. Cell Microbiol. 2007; 9:2689–2699. [PubMed: 17587330]

Kinyanjui MW, Fixman ED. Cell-penetrating peptides and proteins: new inhibitors of allergic airways disease. Can J Physiol Pharmacol. 2008; 86:1–7. [PubMed: 18418441]

Lally ET, Golub EE, Kieba IR. Identification and immunological characterization of the domain of Actinobacillus actinomycetemcomitans leukotoxin that determines its specificity for human target cells. J Biol Chem. 1994; 269:31289–31295. [PubMed: 7983074]

Lally ET, Hill RB, Kieba IR, Korostoff J. The interaction between RTX toxins and target cells. Trends Microbiol. 1999; 7:356–361. [PubMed: 10470043]

Lally ET, Kieba IR, Sato A, Green CL, Rosenbloom J, Korostoff J, et al. RTX toxins recognize a beta2 integrin on the surface of human target cells. J Biol Chem. 1997; 272:30463–30469. [PubMed: 9374538]

Lally ET, Kieba IR, Taichman NS, Rosenbloom J, Gibson CW, Demuth DR, et al. Actinobacillus actinomycetemcomitans leukotoxin is a calcium-binding protein. J Periodontal Res. 1991; 26:268–271. [PubMed: 1831850]

Lear JD, Furblur UG, Lally ET, Tanaka JC. *Actinobacillus actinomycetemcomitans* leukotoxin forms large conductance, voltage-gated ion channels when incorporated into planar lipid bilayers. Biochim Biophys Acta. 1995a; 1238:34–41. [PubMed: 7544624]

Lear JD, Karakelian D, Furblur U, Lally ET, Tanaka JC. Conformational studies of *Actinobacillus actinomycetemcomitans* leukotoxin: partial denaturation enhances toxicity. Biochim Biophys Acta. 2000a; 1476:350–362. [PubMed: 10669799]

Lear JD, Furblur UG, Lally ET, Tanaka JC. *Actinobacillus actinomycetemcomitans* leukotoxin forms large conductance, voltage-gated ion channels when incorporated into planar lipid bilayers. Biochimica et Biophysica Acta. 1995b; 1238:34–41. [PubMed: 7544624]

Lear JD, Karakelian D, Furblur U, Lally ET, Tanaka JC. Conformational studies of *Actinobacillus actinomycetemcomitans* leukotoxin: partial denaturation enhances toxicity. Biochimica et Biophysica Acta (BBA) - Protein Structure and Molecular Enzymology. 2000b; 1476:350–362.

Li JD, Carroll J, Ellar DJ. Crystal structure of insecticidal delta-endotoxin from Bacillus thuringiensis at 2.5 A resolution. Nature. 1991; 353:815–821. [PubMed: 1658659]

Manavalan P, Johnson WC Jr. Variable selection method improves the prediction of protein secondary structure from circular dichroism spectra. Anal Biochem. 1987; 167:76–85. [PubMed: 3434802]

Martin C, Requero MA, Masin J, Konopasek I, Goni FM, Sebo P, Ostolaza H. Membrane restructuring by Bordetella pertussis adenylate cyclase toxin, a member of the RTX toxin family. J Bacteriol. 2004; 186:3760–3765. [PubMed: 15175289]

Menestrina G, Mackman N, Holland IB, Bhakdi S. *Escherichia coli* haemolysin forms voltage-dependent ion channels in lipid membranes. Biochim Biophys Acta. 1987; 905:109–117. [PubMed: 2445378]

Olson F, Hunt CA, Szoka FC, Vail WJ, Papahadjopoulos D. Preparation of liposomes of defined size distribution by extrusion through polycarbonate membranes. Biochim Biophys Acta. 1979; 557:9–23. [PubMed: 95096]

Osickova A, Masin J, Fayolle C, Krusek J, Basler M, Pospisilova E, et al. Adenylate cyclase toxin translocates across target cell membrane without forming a pore. Mol Microbiol. 2010; 75:1550–1562. [PubMed: 20199594]

Parker MW, Pattus F, Tucker AD, Tsernoglou D. Structure of the membrane-pore-forming fragment of colicin A. Nature. 1989; 337:93–96. [PubMed: 2909895]

Paturel L, Casalta JP, Habib G, Nezri M, Raoult D. *Actinobacillus actinomycetemcomitans* endocarditis. Clin Microbiol Infect. 2004; 10:98–118. [PubMed: 14759235]

Sirinian G, Shimizu T, Sugar C, Slots J, Chen C. Periodontopathic bacteria in young healthy subjects of different ethnic backgrounds in Los Angeles. J Periodontol. 2002; 73:283–288. [PubMed: 11922257]

Sreerama N, Woody RW. Estimation of protein secondary structure from circular dichroism spectra: comparison of CONTIN, SELCON, and CDSSTR methods with an expanded reference set. Anal Biochem. 2000; 287:252–260. [PubMed: 11112271]

Stepanovic S, Tosic T, Savic B, Jovanovic M, K'ouas G, Carlier JP. Brain abscess due to *Actinobacillus actinomycetemcomitans*. APMIS. 2005; 113:225–228. [PubMed: 15799768]

Tang G, Kitten T, Munro CL, Wellman GC, Mintz KP. EmaA, a potential virulence determinant of *Aggregatibacter actinomycetemcomitans* in infective endocarditis. Infect Immun. 2008; 76:2316–2324. [PubMed: 18347033]

Tsai CC, Shenker BJ, DiRienzo JM, Malamud D, Taichman NS. Extraction and isolation of a leukotoxin from *Actinobacillus actinomycetemcomitans* with polymyxin B. Infect Immun. 1984; 43:700–705. [PubMed: 6319288]

Uversky VN. Natively unfolded proteins: a point where biology waits for physics. Protein Sci. 2002; 11:739–756. [PubMed: 11910019]

Weinreb PH, Zhen W, Poon AW, Conway KA, Lansbury PT Jr. NACP, a protein implicated in Alzheimer's disease and learning, is natively unfolded. Biochemistry. 1996; 35:13709–13715. [PubMed: 8901511]

Whitmore L, Wallace BA. Protein secondary structure analyses from circular dichroism spectroscopy: methods and reference databases. Biopolymers. 2008; 89:392–400. [PubMed: 17896349]

Wright PE, Dyson HJ. Intrinsically unstructured proteins: re-assessing the protein structure-function paradigm. J Mol Biol. 1999; 293:321–331. [PubMed: 10550212]

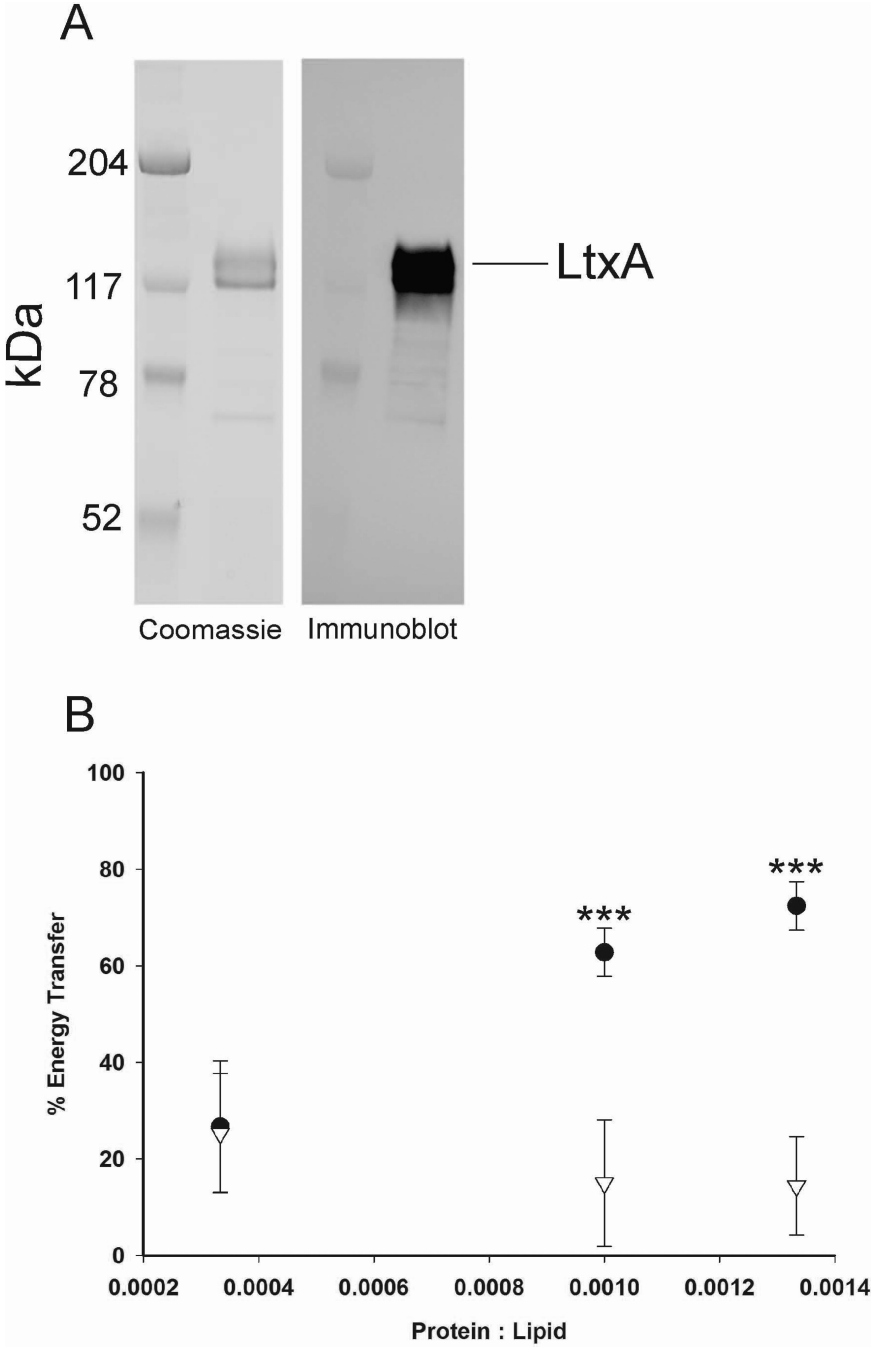

Fig. 1.

LtxA association with lipids and subsequent restructuring. (A) Coomassie stain and immunoblot of purified LtxA. (B) LtxA association with liposomes composed of DMPC/MPC (●) and DMPC/DMPE (∇). (*** $p < 0.001$)

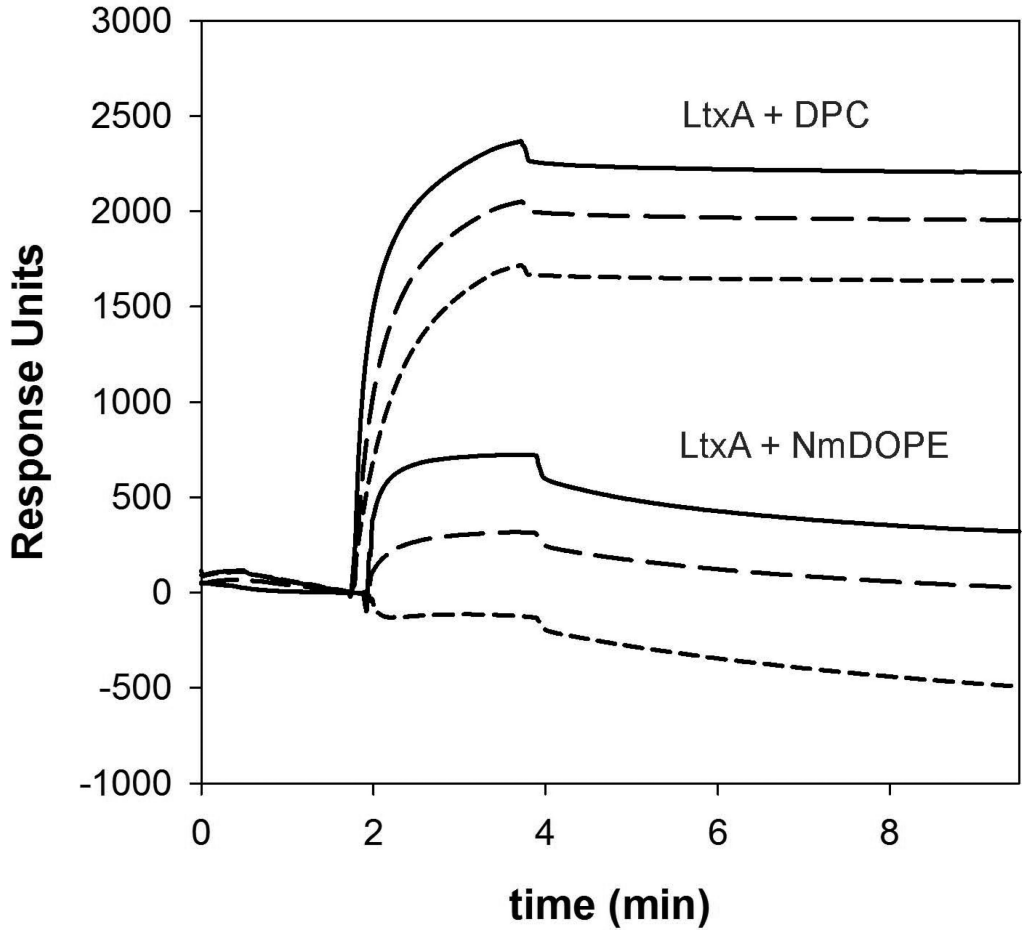

Fig. 2.

Sensorgrams showing LtxA association with DPC or N-m-DOPE at LtxA concentrations of 500 nM (▬▬▬▬▬▬), 250 nM (▬▬ ▬▬), and 125 nM (■ ■ ■ ■ ■ ■ ■).

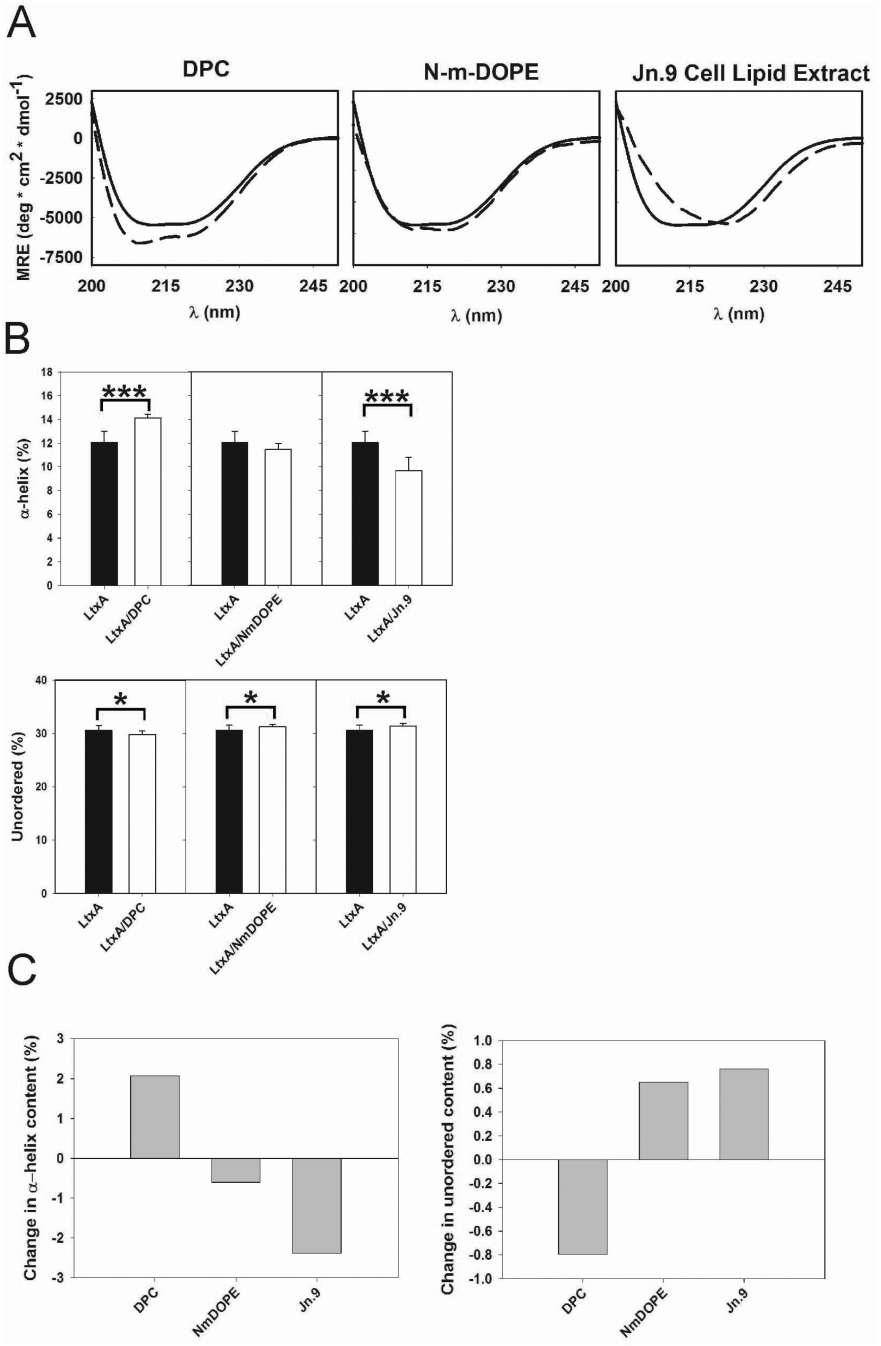

Fig. 3.

Lipid-dependent structural changes in LtxA. (A) CD spectra of LtxA in solution (solid lines) and LtxA incubated with DPC, N-m-DOPE, and Jn.9 cell extracted lipids (dashed lines), at protein:lipid molar ratios of 2×10^{-4}. The plotted curves are the averages of identical repeated samples (n = 3, as described in the Experimental section). (B) Deconvoluted CD spectra from (A) including α-helices and unordered content. (C) Changes in α-helical and unordered content. (*** $p < 0.001$, * $p < 0.05$).

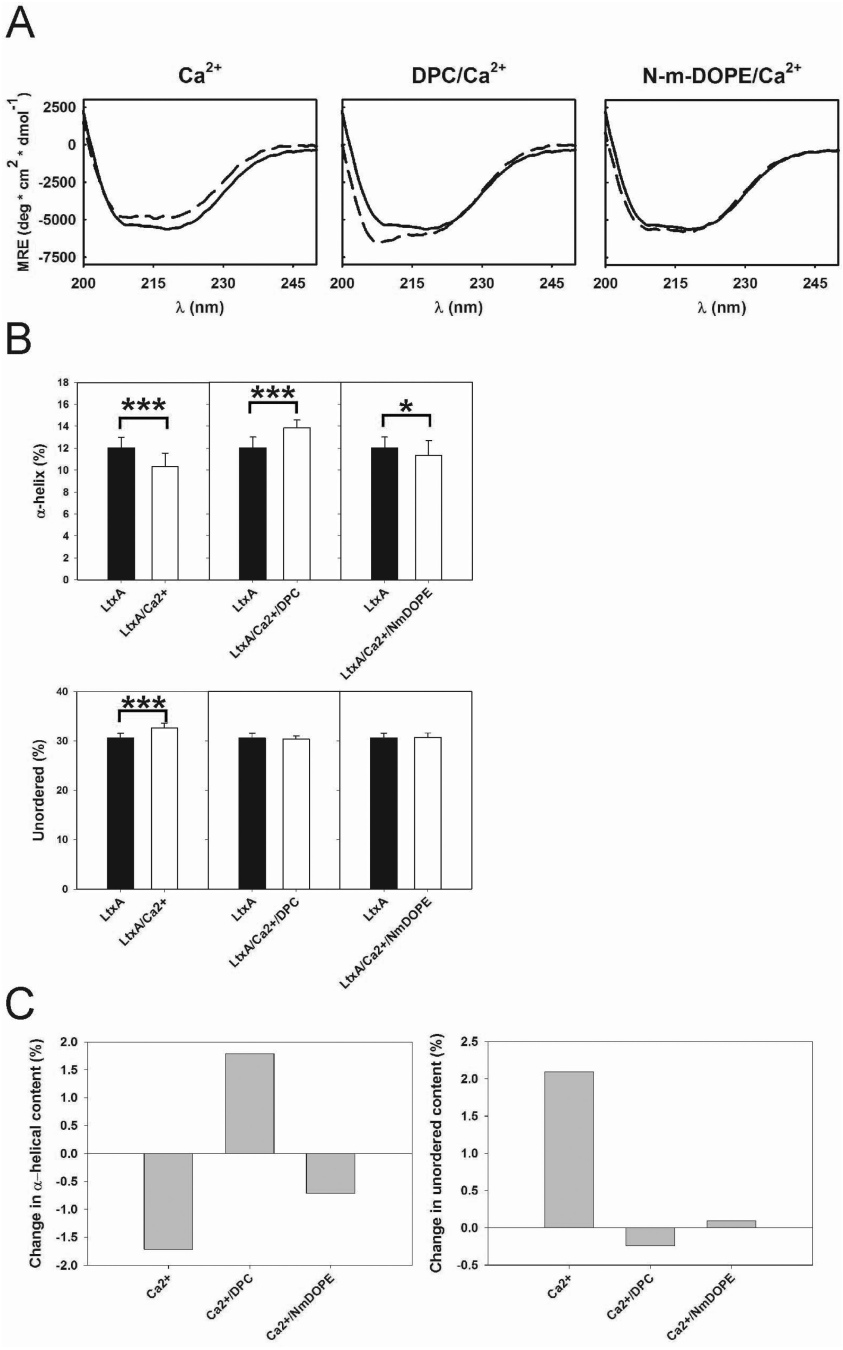

Fig. 4.

Ca^{2+}- and lipid-dependent structural changes in LtxA. (A) CD spectra of LtxA in solution (solid lines) and LtxA incubated with 9 mM Ca^{2+}, 9 mM DPC/Ca^{2+}, and N-m-DOPE/9 mM Ca^{2+} (dashed lines), at protein:lipid molar ratios of 2×10^{-4}. The plotted curves are the averages of identical repeated samples (n = 3, as described in the Experimental section). (B) Deconvoluted CD spectra from (A) including α-helices and unordered content. (C) Changes in α-helical and unordered content. (*** $p < 0.001$, * $p < 0.05$).

Table 1

Kinetics of LtxA Binding to Liposomes composed of DPC and N-m-DOPE. The affinity of LtxA for DPC is stronger (by roughly 8 orders of magnitude) than its affinity for N-m-DOPE.

Lipid	k_a ($M^{-1}s^{-1}$)	k_d (s^{-1})	K_D (M)
DPC	$9.5 (\pm 0.6) \times 10^{4}$	$3.7 (\pm 3.5) \times 10^{-7}$	$3.8 (\pm 3.4) \times 10^{-12}$
N-m-DOPE	$4.5 (\pm 3.8) \times 10^{1}$	$1.1 (\pm 0.1) \times 10^{-3}$	$2.3 (\pm 0.6) \times 10^{-5}$

Table 2

Trp Intensity Changes Upon Incubation with Liposomes Composed of DPC or N-m-DOPE.

Protein:Lipid	DPC	N-m-DOPE
0.00200	0.8540 ± 0.0326	0.8270 ± 0.0174
0.00100	0.7794 ± 0.0402	0.6980 ± 0.0120
0.00067	0.7129 ± 0.0355	0.6510 ± 0.0202
0.00050	0.6733 ± 0.0369	0.5970 ± 0.0075
0.00040	0.6361 ± 0.0261	0.5699 ± 0.0035
0.00033	0.6175 ± 0.0445	0.5365 ± 0.0094
0.00029	0.6053 ± 0.0373	0.4957 ± 0.0032
0.00025	0.5934 ± 0.0581	0.4886 ± 0.0026
0.00022	0.5897 ± 0.0472	0.4847 ± 0.0158

When LtxA was added to 5 mM liposome suspensions of either DPC or N-m-DOPE, a decrease in Trp intensity was observed for all protein:lipid ratios (which ranged from 2×10^{-4} to 2×10^{-3}), indicating that one or more of the Trp residues moved toward a more hydrophilic region and suggesting that LtxA adopted an active conformation.

Table 3

Deconvoluted structural components of LtxA +/- lipids and/or Ca^{2+} [a]

	α-helix (%)	Standard Deviation	Unordered (%)	Standard Deviation
LtxA	12.0	1.0	30.6	0.9
9 mM Ca^{2+}	10.3*	1.2	32.7*	1.0
DPC	14.1*	0.3	29.8***	0.7
DPC/9 mM Ca^{2+}	13.8*	0.7	30.3	0.7
N-m-DOPE	11.4	0.5	31.2***	0.4
N-m-DOPE /9 mM Ca^{2+}	11.3***	1.4	30.7	0.9
Jn.9	9.7*	1.1	31.3***	0.5

*** $p < 0.001$

* $p < 0.05$